



# Simulation on Flyrock due to Blasting Using Smoothed Particle Hydrodynamics (SPH) with LS-Dyna software

Bao Tran DINH<sup>1)\*</sup>, Trieu Do VAN<sup>3)</sup>, Viet Pham VAN<sup>2)</sup>, Nguyen Dinh AN<sup>4)</sup>

<sup>1)</sup> Hanoi University of Mining and Geology, 18 Vien street, Hanoi 100000, Vietnam; Innovations for Sustainable and Responsible Mining (ISRM) Research Group, Hanoi University of Mining and Geology, 18 Vien street, Hanoi 100000, Vietnam; email: trandinhbao@humg.edu.vn, <https://orcid.org/0000-0003-1801-1165>

<sup>2)</sup> Hanoi University of Mining and Geology, 18 Vien street, Hanoi 100000, Vietnam; Innovations for Sustainable and Responsible Mining (ISRM) Research Group, Hanoi University of Mining and Geology, 18 Vien street, Hanoi 100000, Vietnam; email: phamvanviet@humg.edu.vn, <https://orcid.org/0009-0003-3345-9328>

<sup>3)</sup> Institute of Mining Science and Technology – Vinacom; dovantrieu15091996@gmail.com, <https://orcid.org/0009-0007-7887-9034>

<sup>4)</sup> Hanoi University of Mining and Geology, 18 Vien street, Hanoi 100000, Vietnam; Innovations for Sustainable and Responsible Mining (ISRM) Research Group, Hanoi University of Mining and Geology, 18 Vien street, Hanoi 100000, Vietnam; email: nguyendinhhan@humg.edu.vn, <https://orcid.org/0009-0003-2156-6011>

\* Corresponding author: trandinhbao@humg.edu.vn

<http://doi.org/10.29227/IM-2023-02-08>

Submission date: 18-08-2023 | Review date: 11-09-2023

## Abstract

*In surface mining operation, blasting method has been commonly used and accounted highly for breaking waste rock and mineral. The main goal of the activity is fundamental fragmentation by energy generation due to blasting. However, only 20% to 30% blasting energy is generated to fragment rock. The remain energy is wasted for flyrock, ground vibration, air overpressure, dust and too fine fragmentation. Flyrock in blasting is large risk for surface mines and occupies more than a half of incidents relating to blasting at surface mines, because this is a severe issue and causes negative reaction of the surrounding residents. However, studies on flyrock-phenomenon prediction methods for blasting in Vietnam have been also limited. In the study, simulation analysis method on induce-blasting-induced flyrock experiment using Smoothed Particle Hydrodynamics (SPH) with LS-Dyna software. Two-dimension modelling was built and practically applied for B2 cross section of Mong Son quarry in Yen Bai province. The result showed that the ability of Smoothed Particle Hydrodynamics (SPH) in analyzing flyrock trajectory distance in blasting. By using the modelling with field-site parameters, the researcher monitored flyrock velocity at installed time periods, such as 1.5 second when the flyrocks fly with a maximum distance of 85 m from blasting site and their average velocity of 40 m/s.*

**Keywords:** flyrock, smoothed particle hydrodynamics, simulation, blasting, LS-Dyna

## 1. Introduction

In open-pit mining, the blasting method (Blasting) is widely used and has a significant proportion in breaking rocks and extracting valuable minerals. Blasting is the initial and crucial technological step in the mining process, directly influencing the effectiveness of subsequent technological stages.

The main objective of blasting is to efficiently break rocks and extract valuable minerals while ensuring the optimal quality of fragmentation with the lowest possible cost and minimal negative impact on the surrounding environment [1, 2, 3, 4, 5]. To achieve these goals, accurate calculation of the design parameters for blasting and the application of modern blasting techniques are necessary. The blasting operation must fulfill the requirements for the volume of rocks to be broken, the size of rock fragments according to production needs, cost optimization for the entire mining operation, and the minimization and control of harmful effects on the environment. In summary, optimizing the degree of rock fragmentation, displacement distance, geometric size of rock piles after blasting, while ensuring safety in terms of ground vibrations, airblast waves, and flyrock, is the primary objective in any blasting operation.

In the process of blasting operations, it should be noted that only 20% to 30% of the blasting energy is utilized for rock fragmentation. The remaining energy is wasted in the form

of flyrock, ground vibrations, airblast waves, dust generation, and excessive fragmentation [6, 7, 8, 9]. Flyrock is the most significant hazard in open-pit mining blasting operations. It accounts for about half of all mining-related accidents. A study [10] has shown that over 40% of fatal accidents and over 20% of serious accidents in mining operations in India are caused by flyrock. Another study [11] revealed that flyrock exceeding the hazardous zone is the cause of 25% of open-pit mining accidents in the United States. According to statistical accident data [12], flyrock is responsible for 20–40% of mining-related accidents. The dangers and damages caused by flyrock are a serious issue that has been present since the use of blasting in mining operations. Some consequences of flyrock include severe injuries or fatalities, damages to structures and equipment, and even mine closures.

The causes of flyrock phenomenon in mining blasting can include both controllable and uncontrollable factors. Inaccurate blasting design parameters, improper stemming, insufficient burden height, inaccurate hole spacing, excessive explosive charges, unfavorable geological conditions (such as fractures, voids, layering, weak geological formations, etc.), time delays and sequencing inconsistencies, rock fractures and falls, [10, 11, 13, 14], are some of the causes leading to flyrock phenomenon. Therefore, efforts to prevent conditions

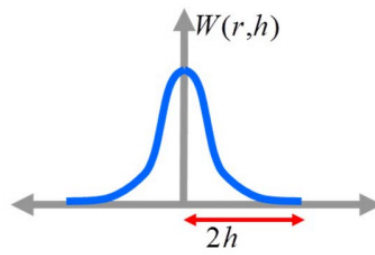


Fig. 1. Interpolation position of kernel function 2D [42]

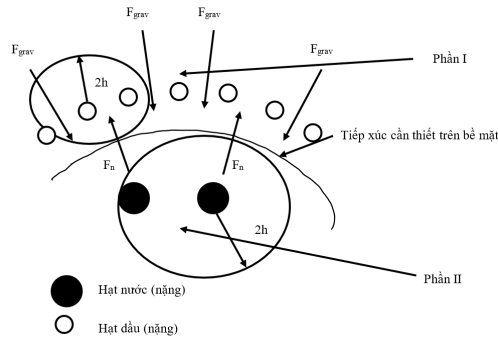


Fig. 2. Particle-particle interactions [43]

that may lead to flyrock phenomenon are an urgent issue that needs to be addressed in current research.

Currently, mining operations are expanding closer to residential areas, increasing the safety risks associated with blasting activities. If issues related to blasting, such as ground vibrations, airblast waves, dust, and especially flyrock, are not properly controlled, they can lead to severe consequences. Until now, many researchers have attempted to predict blasting-related issues through various experimental equations [22, 23]. However, the performance of these models has been unsatisfactory on a large scale, resulting in inaccuracies and a lack of scientific basis. In recent years, various modeling techniques have been applied to predict flyrock distances. Monjezi et al. [24, 25, 26], Rezaei et al. [27], and Ghasemi et al. [28, 29] have utilized artificial neural networks and fuzzy logic techniques for flyrock prediction. Amini et al. [30] employed a machine learning technique called Support Vector Machine (SVM). Raina et al. [31] used a probabilistic method to delineate the hazardous area of flyrock in an open-pit mine. With the emergence of scientific tools, engineering techniques, and advancements in hardware and software in recent decades, the accuracy of predictions has improved [32]. Lastly, the use of AI techniques, including data training and testing from blasting events and comparing results using different algorithms, has gained significant importance in the past decade. AI techniques such as Fuzzy Inference System (FIS), Artificial Neural Networks (ANN), and Adaptive Network-based Fuzzy Inference System (ANFIS) have been successfully applied to solve complex geotechnical problems [33, 34]. These methods have been widely used to mitigate blasting-related issues [35, 36] as AI analysis models leverage the flexible nature of data, allowing easy adjustments as a predictive tool for any new data. This advantage makes AI a fast and powerful tool in addressing non-linear relationships between input and output parameters that are not well-known [37]. However, alongside these advantages, models using AI techniques require a large amount of input data, and measuring flyrock distances from

blasting events is complex and challenging. To date, there has been limited research on using simulation models to predict flyrock phenomena in blasting operations.

In this study, a new method is proposed to predict flyrock distances. The model is developed based on the Smoothed Particle Hydrodynamics (SPH) method, originally developed by Lucy, Gingold, and Monaghan (1977). This method was developed to overcome limitations encountered in extreme deformation problems through the finite element method. The main difference between SPH and conventional methods is that SPH does not divide the nodes. The particles represent the elements that have both general and specific characteristics depending on the declared properties [38, 39].

Until now, several studies have explored the application of the SPH method in simulating blasting operations using LS-Dyna software. Among them, the studies by Jing Gao et al. [40] on "2D Simulation of Blasting Process with 5 Blastholes under Various Horizontal Pressure Coefficients" and Gaohui Wang et al. [41] on "Assessment of Blast Protection and Dam Safety against Explosion Energy" can be mentioned.

Today, simulation has become a reliable solution for studying, analyzing, and evaluating mechanical impact models. This paper performs a simulation analysis of flyrock resulting from blasting using the SPH method in the LS-Dyna software for a 2D model constructed from the B2 cross-section of the Mông Sơn limestone quarry. The results of the model demonstrate the capability of the SPH method in analyzing the details of blasting operations. South-central Vietnam is situated in the Indochina block of Southeast Asia and abundantly occurs Cretaceous granitic batholiths [1–3]. The formation of Cordilleran-type granitic batholiths mainly shows a close correlation with the subduction of oceanic crust beneath the continental crust, and they can be products of crustal recycling and the presence of liquid water [4–11]. Generally, cordilleran granitic batholiths consist of different chemical characterizations due to they are formed by melting of sedimentary rocks (i.e., S-type granites), differentiation



Fig. 3. The border of Mong Son mine [46]

of mafic parental magmas (i.e., A-type granites), and partial melting of dehydrated middle/lower crust (i.e., I-type granites) [11–13]. In south-central Vietnam, granitic batholiths have been considered to be contemporaneous with the granitoid of the South China block. However, only a few studies were carried out on granitic batholiths in this area for investigating Cretaceous magmatism and granite composition [2, 14, 16, 17, 18]. Therefore, Cretaceous magmatism and the formation of granitic batholiths (subducted material (basalt + sediment) or melted basement rock) is still unclear. In this study, granitic rocks of the Deoca, Ankrøet, and Dinhquan complexes are collected for zircon U–Pb analysis to investigate Cretaceous magmatism and granite composition in south-central Vietnam.

## 2. Research Methods

In this section, the authors will provide an overview of the Smoothed Particle Hydrodynamics (SPH) method, the interaction between particles in SPH, as well as the constitutive equation of materials specific to rocks and explosives for simulating blasting operations on a 2D model.

### 2.1. Standard formula of fine particle dynamics (SPH) method

The SPH method is expressed based on the second-order formula of moving particles ( $x_i(t)$ ,  $w_i(t)$ ) for  $i \in P$ , where  $P$  is the set of particles,  $x_i(t)$  represents the position of the  $i$ -th particle, and  $w_i(t)$  denotes the weight of the  $i$ -th particle. The second-order formula for a function can be written as follows:

$$\int_{\Omega} f(x) dx = \sum_{j \in P} w_j(t) \cdot f(x_j(t)) \quad (1)$$

The second-order formula (1), along with the smoothing kernel, forms the definition of an approximate value function for the particles. The interpolated value of the function  $u(x)$  at position  $x$  using the SPH method is given by:

$$\Pi^h(u(x_i)) = \sum_{j \in \Omega} w_j(t) \cdot u(x_j) \cdot w(x_i - x_j, h) \quad (2)$$

Where  $\Sigma$  is taken over all particles within  $\Omega$  and within a radius of  $2h$ ,  $W$  is the position of the smoothing kernel based on the "spline" curve with a radius of  $2h$ , and  $h$  is the

smoothing length in both time and space. The kernel function is defined as follows:

$$w(x_i - x_j, h) = \frac{1}{h} \theta \left\{ \frac{x_i - x_j}{h(x, y)} \right\} \quad (3)$$

$W(x_i - x_j, h)$  tends to  $\delta$  as  $h$  approaches 0, where  $\delta$  is the Dirac function, and  $h$  is a function of  $x_i$  and  $x_j$ , known as the smoothing length of the kernel function.

The spline curve construction function is defined as follows:

$$\theta(d) = Cx \begin{cases} 1 - \frac{3}{2}d^2 + \frac{3}{4}d^3 & \text{Khi } 0 \leq d \leq 1 \\ \frac{1}{4}(2-d)^3 & \text{Khi } 1 \leq d \leq 2 \\ 0 & \text{Khac} \end{cases} \quad (4)$$

With  $d$  being the spatial dimension, the gradient of the function  $u(x)$  is obtained by applying the derivative operator to the smoothing length:

$$\nabla \Pi^h(u(x_i)) = \sum_j w_j \cdot u(x_j) \cdot \nabla w(x_i - x_j, h) \quad (5)$$

The evaluation of an inner product interpolation of two functions is given by the product of their interpolated values (Fig 1).

### 2.2. Continuity equations and momentum equations of particles in the smoothed particle dynamics method

The approximate value of the particle in the continuity equation is determined as follows:

$$\frac{dp_i}{dt} = \rho_i \sum_j \frac{m_j}{\rho_j} (v_i^s - v_j^s) w_{ij} \beta \quad (6)$$

It is Galilean invariant, as the position and velocity of particles only appear in the form of differences, where is the velocity component at the  $i$ -th particle.

The discrete form of the SPH momentum equation is developed as:

$$\frac{dv_i^s}{dt} = - \sum_j \frac{m_j}{\rho_i \rho_j} (\sigma_i^s \pm \sigma_j^s) w_{ij} \beta \quad (7)$$

The formula ensures that the stress is automatically continuous on the material's interface. Different types of SPH

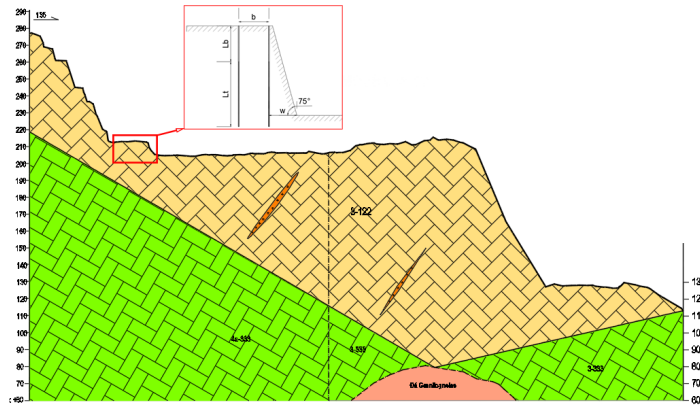


Fig. 4. Section of B2 line of Mong Son mine and explosive loading diagram used to simulate blasting on LS-Dyna software

momentum equations can be achieved by applying different consistency equations to the standard SPH momentum equation. The symmetry of the SPH momentum equation helps to reduce errors arising from particle inconsistency issues.

From equation (7), the components of the forces acting on each particle can be determined.

$$F_i^{\text{pressure}} = -\sum_j m_j \frac{P_i + P_j}{2\rho_j} \nabla W(r_{ij}, h) \quad (8)$$

$$F_i^{\text{viscosity}} = \mu \sum_j m_j \frac{V_i + V_j}{2\rho_j} \nabla^2 W(r_{ij}, h)$$

Where:  $r_{ij} = x_i - x_j$ ,  $\mu$  is the viscosity coefficient of the material. The pressure  $p_i$  is calculated through the equation of state:

$$p_i = k(\rho_i - \rho_0) \quad (9)$$

Where:  $k$  is the stiffness of the material and  $B$  is its initial density. Finally, for the acceleration of particle  $i$ , we have:

$$a_i = \frac{1}{\rho_i (F_i^{\text{pressure}} + F_i^{\text{viscosity}} + F_i^{\text{external}})} \quad (10)$$

where:  $F_i^{\text{external}}$  represents external forces such as forces acting on the body or contact forces.

### 2.3. Interactions between particles in simulation

Fig 2 illustrates that all SPH interpolations are performed within the local domains of each SPH particle. Contact forces will be applied to external forces as described in equation 10.

In this system, the contact force acting on the particles due to contact,  $F_c$ , is proportional to the displacement or overlap between the particles,  $\delta$ .

$$F_c = K_l \delta \quad (11)$$

Where  $\delta = d - 2d$  and  $K_l$  is the linear spring constant or stiffness. If the contact point is modeled using only this linear spring, no energy will be dissipated and the contact will be perfectly elastic. In reality, some kinetic energy is dissipated through plastic deformation, either converted into heat or sound energy. To account for these energy losses, a damping source based on the dashpot model is defined:

$$F_d = \eta v \quad (12)$$

The damping force is proportional to the relative velocity of the contacting particles, where the proportionality constant  $\eta$  is called the damping coefficient,  $v = v_1 - v_2$ .

### 2.4. Characterization equation of the materials used in the simulation

Alongside the development of the SPH method, material models have been constructed and advanced to address issues within the simulation framework of LS-Dyna software. In the scope of studying rock fragmentation caused by blasting, the research group utilizes characteristic models for soil and rock: the Riedel-Hiermaier-Thoma (RHT) model and the High Explosive Burn (HEB) model, which incorporates the Jones-Wilkins-Lee (JWL) stress wave propagation equation for the explosive material.

#### - Rock Material Model (RHT)

The characteristic of rock is its brittle behavior [44]. Therefore, the suitable material model in LS-Dyna is the Riedel-Hiermaier-Thoma (RHT) material model, developed by Riedel, Hiermaier, and Thoma [45]. RHT consists of three pressure-dependent yield surfaces in the stress space, representing different limiting states, namely the yield limit, elastic limit, and ultimate failure limit.

The failure limit  $Y_{\text{phá hủy}}$  is defined as a function of pressure  $p$ , angle  $\theta$ , and strain rate  $\epsilon$ , and is determined by the formula.

$$Y_{\text{phá hủy}}(p^*, \theta, \epsilon) = Y_{\text{TXC}}^*(p^*) \cdot R_3(\theta) \cdot F_{\text{tỉe}}(\epsilon) \quad (13)$$

Where  $p^*$  is the pressure normalized by the function  $f_c$ ,  $p^* = p/f_c$ , where  $p$  is the hydrostatic pressure,  $f_c$  is the compression strength;  $R_3(\theta)$  is a function defining the invariant dependence of a shape;  $F_{\text{strain}}$  is the strain rate, expressed through the increase in fracture toughness with plastic strain rate;  $Y_{\text{TXC}}^*$  is the equivalent stress intensity factor on the compressive meridian.

The elastic limit is determined based on the ratio of the fracture surface area, defined by the formula [9]:

$$Y_{\text{đàn hồi}} = Y_{\text{phá hủy}} \cdot F_{\text{đàn hồi}} \cdot R_3(\theta) \cdot F_{\text{CAP}}(p^*) \quad (14)$$

Where,  $F_{\text{đàn hồi}}$  – the ratio between the elastic limit and the failure limit;  $F_{\text{CAP}}(p^*)$  is the function of the elastic limit deviation stress when subjected to hydrostatic compression, with values in the range (0,1).



Tab. 1. Drilling and blasting parameters on simulation model

Parameters	Symbol	Unit	Value
Bench height	h	m	8
Burden	b	m	2.6
Stemming	L <sub>b</sub>	m	3.2
Explosive Charge	L <sub>t</sub>	m	5.8
Hole Diameter	d <sub>k</sub>	mm	76
Bottom-Hole Burden	w	m	2.6
Type of explosives			Anfo
Delay time		ms	17

Tab. 2. Key parameters of the materials used in the simulation model

Parameters	Values	Parameters	Values
<b>RHT material model</b>			
Mass density, g/cm <sup>3</sup>	2,72	Crush pressure, Pa	4,00e+7
Tensile strength, kg/cm <sup>2</sup>	60,77	Break compressive strain rate	3,00e+19
Compression resistance strength, kg/cm <sup>2</sup>	750,77	Break tensile strain rate	3,00e+19
Angle of internal friction, đ <sup>o</sup>	34 <sup>o</sup> 35'	Reference tensile strain rate	3,00e-6
Deformation modulus, kg/cm <sup>2</sup>	4,08	Reference compressive strain rate	3,00e-5
Elastic modulus, Pa	2,47e+10	Shear modulus reduction factor	0,5
Porosity	1,94	Minimum damaged residual strain	0,015
<b>JWL stress wave equation</b>			
Mass density, kg/m <sup>3</sup>	931	Chapman-Jouget pressure	5,15e+9
Detonation velocity, m/s	4.200		
Equation of state coefficient (A), Pa	4,95e+10	Equation of state coefficient (A), Pa (R2)	1,118
Equation of state coefficient (B), Pa	1,89e+9	Equation of state coefficient (A), Pa (ω)	0,33
Equation of state coefficient (R1)	3,907	Detonation energy per unit volume and initial value for E. See equation in Remarks, Pa, Pa/m <sup>3</sup>	2,48e+9

Secondary fragmentation is used to describe the strength of completely crushed rock, and it is determined by the following expression:

$$Y_{\text{phaluythupha}}^* = B \cdot p^{*M} \quad (15)$$

Where B is the constant of secondary fragmentation, and M is the exponent of secondary fragmentation.

- The stress wave propagation equation of the explosive material (JWL)

For the explosive charge inside the borehole, the high explosive burn (HEB) material model used in LS-Dyna utilizes the Jones-Wilkins-Lee (JWL) stress wave propagation equation, which is defined by the equation [45]:

$$P = A(1 - \frac{\omega}{R_1 V})e^{-R_1 V} + B(1 - \frac{\omega}{R_2 V})e^{-R_2 V} + \frac{\omega E}{V} \quad (16)$$

In which, P represents the stress wave, A, B, R<sub>1</sub>, R<sub>2</sub>, and ω are constants, V is the specific volume, and E<sub>0</sub> is the initial internal energy with a value of E<sub>0</sub>.

### 3. Results and discussions

#### 3.1. Characteristics of the study area

##### a. Geographical location

The Mong Son limestone quarry is located in Mong Son commune, Yen Binh district, Yen Bai province. The total licensed area for zones A and B of the quarry is 13.9 hectares (Fig. 3). The geological structure of the mining area is relatively simple, primarily consisting of white weathered limestone. The limestone is pure white with a fine crystalline structure and relatively large particle size.

##### b. The current state of mining technology and drilling and blasting operations at the Mong Son limestone quarry [47]

The Mong Son quarry is currently focused on mining Area A, which covers an area of 11.81 hectares. The mining method employed is layer-by-layer extraction from top to bottom, with each layer being 8.0 meters in height. The slope angle of the layers is α = 75<sup>o</sup>. The rock in the quarry is fragmented using the drilling and blasting method, with drill holes having a diameter of 76 mm. The blasting technique used is full electric delay blasting, with delay times of 17 ms and 42 ms. The explosive material used is Anfo in the form of D60 bags, and the emulsion explosive is D60, initiated by a 400ms electric detonator and an MN31-175g booster (for the first mining blast). The majority of the explosive charge is continuously structured within the blast column.

#### 3.2. Simulation model of blasting process at B2 section at Mong Son limestone quarry using LS-Dyna software

Currently, at some production blasting sites in the quarry, the applied drilling and blasting parameters have increased the risk of flyrock hazards. Therefore, in order to assess the impact of flyrock on production, the paper conducted a simulation of the blasting process using LS-Dyna software on the cross-sectional profile B2 of the quarry (Fig. 4).

The drilling parameters on the 2D model are presented in Tab. 1.

The materials representing the geological environment, as well as the explosives compatible with the properties of RHT and JWL materials in LS-Dyna, are determined based on the geological data of the Mong Son limestone quarry and existing studies on the mechanical properties of limestone with a density of 2.72 g/cm<sup>3</sup>. The key parameters of the materials are shown in Tab. 2.

The computer specifications used for simulating the blasting work are as follows: Intel(R) Core(TM) i7-10700 CPU @ 2.90GHz and 16.0 GB of RAM. With a result recording time

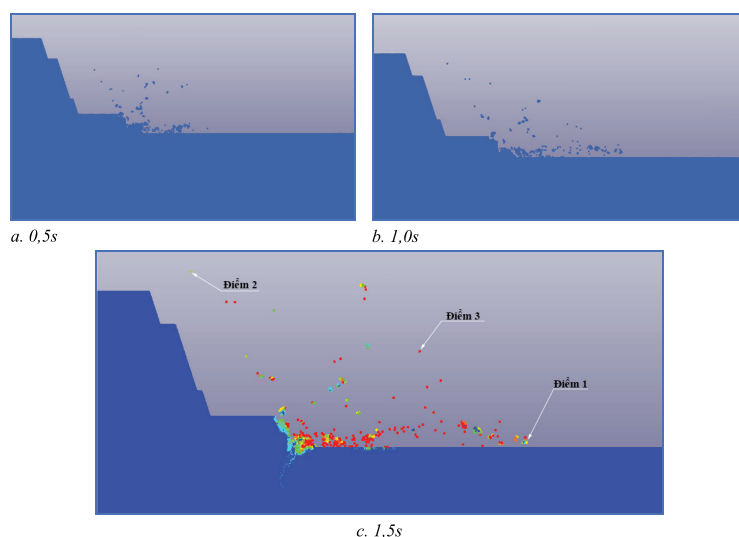


Fig. 5. Simulation of the blasting process using LS-Dyna software

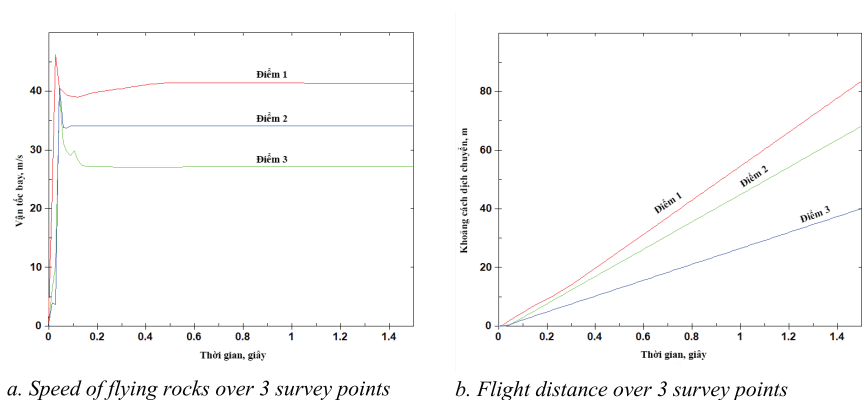


Fig. 6. Velocity (a) and distance (b) flying from 0 ÷ 1.5 seconds

of 1.5 seconds, the simulation completed its calculations after 12 hours using the LS-Dyna software.

### 3.3. Simulation results of flying rock for Mong Son limestone quarry by SPH method on LS-Dyna software

The article sets up data measurements for simulating the rock fragmentation phenomenon during the blasting process on a 2D model of cross-section B2 at Mong Son limestone quarry after 1.5 seconds. The obtained results are recorded at time intervals of 0.5 seconds, 1.0 second, and 1.5 seconds, as shown in Fig. 5.

To assess the distance of flyrock and the velocity of flyrock after 1.5 seconds of detonating the explosive charge, three measurement points were set in the simulation model (Fig.5c). The monitoring results are presented in Fig. 6.

The measurement results at the monitoring points show that with the blast network parameters as shown in Tab.1, after 1.5 seconds, the farthest flyrock from the blast center reached a distance of 85 meters, corresponding to an average velocity of 40 m/s. Therefore, the blast network parameters pose a potential risk of flyrock hazards for the Mong Son quarry. It is necessary to calculate and select the blast network parameters based on the safe criteria for flyrock.

## 4. Conclusions

The simulation method for the blasting process and the determination of the trajectory and flyrock distance of the

rock and soil using simulation tools is not widely used in our country at present. The use of empirical formulas to determine flyrock distances is not suitable for real blasting conditions, while applying machine learning algorithms and AI models requires collecting a large amount of input parameters. On the other hand, measuring and documenting flyrock distances caused by blasting events is extremely complex and challenging.

Numerical modeling methods have become a reliable solution for studying, analyzing, and evaluating mechanical impacts. The results of the model demonstrate the capabilities of the Smoothed Particle Hydrodynamics (SPH) method in analyzing blasting operations in depth. The use of this method enables mining engineers and safety managers to preliminarily predict flyrock distances for each blast under realistic blasting conditions at the mine by inputting the required simulation parameters.

Based on the analysis of the blasting effects using the 2D SPH method constructed from the B2 cross-section of the Mông Sơn limestone quarry, it is evident that the current design parameters for the blast network (KNM) pose a potential risk of flyrock hazards. Therefore, it is necessary to further study, calculate, and select appropriate KNM parameters. However, more detailed and in-depth research is required on the application of the SPH method in LS-Dyna software for 3D models with multiple realistic blastholes according to ac-

tual construction plans and supplementary experiments that consider additional mechanical properties specific to the rock and soil characteristics at the quarry. This will enhance the accuracy of the simulations and establish longer observation periods to fully understand the flyrock phenomena in different directions and at different time points during the blasting events.

## 5. Acknowledgements

The authors would like to sincerely thank Assoc. Prof. Dr. Dam Trong Thang from the Military Technical Acad-

emy for his assistance during the simulation of the mining blasting using the licensed software LS-Dyna/Ansys. Additionally, the authors express their gratitude for the support and scientific advice provided by the scientists from the Strong Research Group "Advancements in Sustainable and Responsible Mining" – ISRM, during the execution of this research.

The paper was presented during the 6th VIET-POL International Conference on Scientific-Research Cooperation between Vietnam and Poland, 10-14.11.2021, HUMG, Hanoi, Vietnam.

## Literatura – References

1. Kahrman, A., Ozer, U., Aksoy, M., Karadogan, A., Tuncer, G. (2006). Environmental impacts of bench blasting at Hisarcik Boron open pit mine in Turkey. *Environmental Geology*, 50 (7), 1015-1023.
2. Uysal, O., Cavus, M. (2013). Effect of a pre-split plane on the frequencies of blast induced ground vibrations. *Acta Montanistica Slovaca*, 18(2), 101-109.
3. Karadogan, A., Kahrman, A., Ozer, U. (2014). A new damage criteria norm for blast induced ground vibrations in Turkey. *Arabian Journal of Geosciences*, 7(4), 1617-1627.
4. Gorgulu, K., Arpaz, E., Uysal, O., Duruturk, Y.S., Yuksek, A.G., Kocaslan, A., Dilmac, M.K. (2015). Investigation of the effects of blasting design parameters and rock properties on blast-induced ground vibrations. *Arabian Journal of Geosciences*, 8(6), 4269- 4278.
5. Kulekci, G., Alemdag, S. (2016). The investigation of blasting effect on natural heritages in quarries: Registered rock room sample. *Proceedings of the 8th International Aggregates Symposium*, 13-14 October, Kutahya, Turkey, 498-504.
6. Singh, T.N., Singh, V. (2005). An intelligent approach to prediction and control ground vibration in mines. *Geotechnical and Geological Engineering*, 23(3), 249-262.
7. Rezaei, M., Monjezi, M., Varjani, A.Y. (2011). Development of a fuzzy model to predict flyrock in surface mining. *Safety Science*, 49, 298-305.
8. Hajihassani, M., Armaghani, D.J., Sohaei, H., Mohamad, E.T., Marto, A. (2014). Prediction of airblast-overpressure induced by blasting using a hybrid artificial neural network and particle swarm optimization. *Applied Acoustics*, 80, 57-67.
9. Sadeghi, F., Monjezi, M., Armaghani, D.J. (2020). Evaluation and optimization of prediction of toe that arises from mine blasting operation using various soft computing techniques. *Natural Resources Research*, 29(2), 887-903.
10. Bhandari S (1997) *Engineering rock blasting operations*. A. A. Balkema, Rotterdam.
11. Fletcher, L. R., D'Andrea, D. V. (1986): Control of flyrock in blasting. *Proc., 12th Conf. on Explosives and Blasting Technique*, Atlanta, Georgia, 167-177.
12. Raina AK, Murthy VMSR, Soni AK (2015) Flyrock in surface mine blasting: understanding the basics to develop a predictive regime. *Curr Sci* 108:660–665.
13. Workman, J. L., Calder, P. N. (1994): Flyrock prediction and control in surface mine blasting. *Proc., 20th Conf. on Explosives and Blasting Technique*, Austin, Texas, 59-74.
14. Kopp, J. W. (1994): Observation of flyrock at several mines and quarries. *Proc., 20th Conf. on Explosives and Blasting Technique*, Austin, Texas, 75-81.
15. Lundborg N, Persson PA, Ladegaard-Pedersen A, Holmberg R (1975) keeping the lid on flyrock in opencast blasting. *Eng Min J* 95–100.
16. Roth J (1979) A model for the determination of flyrock range as a function of shot conditions, final report contract no. J03872A2. *Management Science Associates*, Los Altos.
17. Hillier DE, Holywell PD, Jeffries RM, Scott IMB (1999) Limiting the instance of flyrock from quarry operations, research report. *WS Atkins Consultants Ltd.*, Warrington.

18. Schneider L (1997) Back to the basics, flyrock (part 2: prevention). *The Journal of explosives engineering* 14:1–14 quarry blasting. *Appl Acoust* 71:1169–1176. doi:10.1016/j.apacoust.2010.07.008
19. Adhikari GR (1999) Studies on flyrock at limestone quarries. *Rock Mech Rock Eng* 32:291–301. doi:10.1007/s006030050049
20. Mishra AK, Mallick DK (2012) Analysis of blasting related accidents with emphasis on flyrock and its mitigation in surface mines. In: *Proceedings of the 10th International Symposium on Rock Fragmentation by Blasting*, New Delhi, India. pp. 555–563
21. Bajpayee TS, Rehak TR, Mowrey GL, Ingram DK (2004) Blasting injuries in surface mining with emphasis on flyrock and blast area security. *J Saf Res* 35:47–57. doi:10.1016/j.jsr.2003.07.00
22. Kulekci, G., Yilmaz, A.O. (2018). Roadway tunnel construction with drilling-blasting method; Gümüşhane environment road example. *Int. Journal on Mathematic, Engineering and Natural Sciences*, 4, 34-39.
23. Kulekci, G., Yilmaz, A. (2019). Investigation of the effect of activities in a copper mine on historical works, an example of Gümüşhane Süleymaniye. *Journal of Underground Resources*, 16(8), 1-14.
24. Monjezi, M., Amini Khoshalan, H., Yazdian Varjani, A. (2010a). Prediction of flyrock and backbreak in open pit blasting operation: a neuro-genetic approach. *Arabian Journal of Geosciences*, 5(3), 441-448.
25. Monjezi, M., Bahrami, A., Yazdian Varjani, A. (2010b). Simultaneous prediction of fragmentation and flyrock in blasting operation using artificial neural networks. *International Journal of Rock Mechanics and Mining Sciences*, 47(3), 476-480.
26. Monjezi, M., Mehrdanesh, A., Malek, A., Khandelwal, M. (2012). Evaluation of effect of blast design parameters on flyrock using artificial neural networks. *Neural Computing and Applications*, 23(2), 349-356.
27. Rezaei, M., Monjezi, M., Varjani, A.Y. (2011). Development of a fuzzy model to predict flyrock in surface mining. *Safety Science*, 49, 298-305.
28. Ghasemi, E., Sari, M., Ataei, M. (2012a). Development of an empirical model for predicting the effects of controllable blasting parameters on flyrock distance in surface mines. *International Journal of Rock Mechanics and Mining Sciences*, 52, 163-170.
29. Ghasemi, E., Amini, H., Ataei, M., Khalokakaei, R. (2012b). Application of artificial intelligence techniques for predicting the flyrock distance caused by blasting operation. *Arabian Journal of Geosciences*, 7(1), 193-202.
30. Amini, H., Gholami, R., Monjezi, M., Torabi, S.R., Zadhesh, J. (2011). Evaluation of flyrock phenomenon due to blasting operation by support vector machine. *Neural Computing and Applications*, 21(8), 2077-2085.
31. Raina, A.K., Chakraborty, A.K., Choudhury, P.B., Sinha, A. (2011). Flyrock danger zone demarcation in opencast mines: a risk based approach. *Bulletin of Engineering Geology and the Environment*, 70(1), 163-172.
32. Alemdag, S., Zeybek, H.I., Kulekci, G. (2019). Stability evaluation of the Gümüşhane-Akçakale Cave by numerical analysis method. *Journal of Mountain Science*, 16(9), 2150-58.
33. Momeni, E., Nazir, R., Armaghani, D.J., Maizir, H. (2014). Prediction of pile bearing capacity using a hybrid genetic algorithm-based ANN. *Measurement*, 57, 122-131.
34. Mohamad, E.T., Armaghani, D.J., Hajihassani, M., Faizi, K., Marto, A. (2013a). A simulation approach to predict blasting-induced flyrock and size of thrown rocks. *Electronic Journal of Geotechnical Engineering*, 18, 365-374.
35. Monjezi, M., Dehghani, H. (2008). Evaluation of effect of blasting pattern parameters on back break using neural networks. *International Journal of Rock Mechanics and Mining Sciences*, 45(8), 1446-1453.
36. Esmaeili, M., Osanloo, M., Rashidinejad, F., Bazzazi, A.A., Taji, M. (2014). Multiple regression, ANN and ANFIS models for prediction of backbreak in the open pit blasting. *Engineering with Computers*, 30(4), 549-558.
37. Garret, J.H. (1994). Where and why artificial neural networks are applicable in civil engineering. *Journal of Computer in Civil Engineering*, 8, 129-130.
38. Tran Thanh Thung. (2017). Study of the SPH method for Simulation in LS-Dyna
39. L.B. Jayasinghe. (2020). Numerical investigation into the blasting-induced damage characteristics of rocks considering the role of in-situ stressed and discontinuity persistence. Nanyang Centre for Underground Space, School of Civil and Environmental Engineering, Nanyang Technological University, Singapore 639798.
40. Jing Gao, Shizhen Xie, Xiantang Zhang, Hongli Wang, Wenle Gao, và Hongmin Zhou. (2020). Study on the 2D optimization simulation of complex five-hole cutting blasting under different lateral pressure coefficients. *Hindawi Complexity*. Volume 2020, Article ID 4639518, 12 pages
41. Gaohui Wang, Sherong Zhang, Yuan Kong, and Hongbi LI. (2013). A comparative study on the dynamic response of concrete gravity dams subjected to underwater and air explosions. *Journal of Performance of Constructed Facili-*



ties. Submitted October 22, 2013; accepted January 29, 2014; posted ahead of print January 31, 2014. doi:10.1061/(ASCE)CF.1943-5509.0000589.

42. Jingxiao Xu, Jason Wang. (2013). Interaction Methods for the SPH Parts (Multiphase Flows, Solid Bodies) in LS-Dyna. Livermore Software Technology Corporation.
43. PGS.TS. Đàm Trọng Thắng, PGS. TS. Bùi Xuân Nam, TS. Trần Quang Hiếu. (2015). Nổ mìn trong ngành mỏ và công trình. NXB Khoa học tự nhiên và công nghệ. Hà Nội
44. Jing Gao, Shizhen Xie, Xiantang Zhang, Hongli Wang, Wenle Gao, và Hongmin Zhou. (2020). Study on the 2D optimization simulation of complex five-hole cutting blasting under different lateral pressure coefficients. Hindawi Complexity. Volume 2020, Article ID 4639518, 12 pages
45. Riedel, W., Thoma, K., Hiermaier, S. (1999). Numerical analysis using a new macroscopic concrete model for hydrocodes. In Proceedings of 9th international symposium on interaction of the effects of munitions with structures (pp. 315–322). Strausberg, Germany
46. Satellite Images of Mong Son quarrz.
47. Illustration of Mining Production Adjustment of Mong Son Quarry, Mong Son Ward, Yen Binh District, Yen Bai Province